Study of the Hydrodynamic Performance of a Compact and Intensified G/L Contactor: the RPB

Usman GARBA,[1,2] , David ROUZINEAU[1] , Michel MEYER[1]

[1] Chemical Engineering Laboratory, University of Toulouse, CNRS, INPT, UPS, Toulouse, France
[2] Usmanu Danfodiyo University Sokoto, Nigeria

Abstract
Modern process equipment needed for safe and economically viable chemical and biological processes requires flexibility, compactness, and a great potential for enhancing mass transfer. Centrifugal process intensification equipment such as the rotating packed bed (RPB) satisfies the above mentioned requirements in addition to zero sensitivity to changes caused by gravity. The fundamental principles of RPBs are yet to be fully established due to difficulty in predicting their behavior which has necessitated the need for treating their design, modeling, and optimization on a case-to-case basis. This study focused on the hydrodynamics (pressure drops) of a pilot-scale RPB equipped with a stainless steel wire mesh packing. The effects of three operational parameters: average high gravity factor, integrated gas capacity factor, and liquid load, as well as a design parameter, the fluid distributor type were investigated. The maximum value of the average gravity factor used was 452. Also, a combined gas capacity factor of 2.6Pa$^{0.5}$, and a liquid load of up to 20m^{3}m^{-2}h^{-1} were explored. Additionally, the influence of liquid distributor type on the pressure drop of RPBs was investigated.

Keywords*: Hydrodynamics, Gas/Liquid Contactor, rotating packed bed, pressure drop, operational parameters*

Introduction

The design, optimization, and scale-up of separation processes are increasingly demanding more robust routes to meet current global realities. Both environmental and socioeconomic demands require newer and more sustainable approaches to converting matter and energy. An essential aspect of the transformation of reacting species and mixtures is their separation into constituent components. Basic fluid separation techniques such as absorption, adsorption, distillation, and extraction, as well as their combinations, are conducted in conventional packed columns. However, conventional packed columns rely on gravity for their operations. Thus, the operating ranges of such columns are limited, and they usually have large sizes and footprints. A RPB, also known as "HiGee" (high gravity), is a gas-liquid contactor in which gravitational force is replaced by centrifugal force in an environment which is about 10 to 1000 folds more than gravity (Groß et al., 2018; Pan et al., 2017). The rapid renewal of the gas-liquid contact surface in RPBs accommodates the use of packings with a large effective area of about 2000-5000m^2/m^3 and with 90 to 95% porosity. This led to reduced liquid film thickness, increased gas-liquid contacting efficiency, hydraulic capacity, and flooding capacity, all of which improve the mass transfer efficiency and led to a compact contactor (Pan et al., 2017). The smaller sizes and higher throughputs of RPBs are important for nautical or process modification purposes (Hilpert & Repke, 2021). Reduced equipment sizes also reduce the fluid residence time, which significantly reduces safety risks, energy and material consumption which directly impact the economy of processes. Compared to conventional packed columns, RPBs offer higher throughputs, better micro-mixing efficiency, a comparable processing capacity and efficiency, provide the foundation of modular plants and the rotation of the rotor as an extra degree of freedom (Neumann et al., 2018).

A comprehensive study of the basic principles is essential to model, design, optimize, commission pilot-scale, and subsequently scale-up RPBs (Hendry et al., 2020; Zhang et al., 2020). This is achievable through systematic hydrodynamic investigations via simulation and modeling studies which can be

verified experimentally (Neumann et al., 2017a). Absorption and stripping, mainly using air-water systems, are the standard methods used to study RPB hydrodynamic variables. Several studies have been conducted to study the hydrodynamic behavior of RPBs. Some recent such studies include an in-depth analysis of the operating limits required to achieve specified RPB capacity (Groß et al., 2018) and the work of Hendry et al., (2020) which detailed the contributions of different zones of the RPB to its overall pressure drop obtained by profiling each zone's internal radial pressure drop. Górak (2015) observed that the fluid dynamics in RPBs are inhomogeneous, the hydrodynamics challenging to predict, and some of its processes (specifically distillation) are yet to be fully established. Even though many of RPBs' numerous applications have been thoroughly researched and documented up to industrial application levels, its design approach is still case-specific, necessitating improvements (Neumann et al., 2017a). Hendry et al., (2020) observed the slowness of improvements in understanding the fundamentals of RPB hydrodynamics. The slow progress necessitates dependence on empirical models, which could affect the validity of scale-up procedures.

In this study, we aim to obtain primary data needed to further enhance the understanding of the basic principles of RPBs via its hydrodynamic characteristics. The main focus of this investigation was the pressure drop as a fundamental hydrodynamics characteristic of a pilot-scale RPB. The effect of basic RPB operating parameters, and that of a design parameter on the pressure drop of the RPB were studied. Two types of nozzles, a double jet nozzle, and a single central distributor, were investigated.

Context

RPBs are classified according to numerous criteria, which include the packing used and its configuration, flow direction(s) of the contacting phases, and the type, number, orientation, and nature of assembly of the rotors used. Detailed descriptions of many types and forms of RPBs have been given by Garcia et al., (2017). A review of the various applications of RPBs up to the industrial scale was done by Neumann et al., (2018). They showed that RPBs had been used for separation processes, pollution control, nanoparticle manufacture, material synthesis, emulsification, polymerization, and sulphonation. Also, RPBs have been employed in various fields such as petroleum product processing, biodiesel production, and medical sciences. A conventional RPB comprises of a shell surrounding a rotor mounted on a vertical or horizontal shaft rotated by a motor. The ring-shaped, motor-driven cylinder, which is the rotor, encloses an annular packing. Fluid contact operation in RPBs can be countercurrent, cocurrent, or crosscurrent (Pan et al., 2017).

In a single-block RPB in countercurrent operation, gas is introduced into the outer periphery of the packing from the shell, as illustrated in Figure 1. The liquid is introduced into the center of the rotor, also called the 'eye,' through the liquid inlet(s) using a stationary liquid distributor into the packing from the topmost part of the RPB. Centrifugal shear forces transform the liquid into rivulets, droplets, or films as dictated by the rotation speed as described by (Burns & Ramshaw, 1996). The liquid is finally collected by the walls of the shell and flows downwards, leaving the casing via the liquid outlet(s).

In conventional packed columns, at a particular gas flow rate, usually expressed as the gas capacity factor (F_G), flooding occurs throughout the column because of the uniform crossection of the column. The phenomenon is characterized by the almost complete filling of the packing pores. This result in a noticeable, steep rise in pressure drop. However, due to the rotor geometry, the crossectional area of RPB packings varies along the radius. This variation in the crossectional area makes the highest relative velocities between gas and liquid, and the lowest relative centrifugal force, otherwise known as the high gravity factor, exists at the center of the packing (Groß et al., 2020; Neumann et al., 2017a). Consequently, since flooding in RPBs emanate from the center of the packing where the liquid is injected, a noticeable sharp rise in the total pressure drop or liquid hold-up may not occur. Hence, changes in pressure drop at flooding points in RPBs are inconsistent (Hendry et al., 2020).

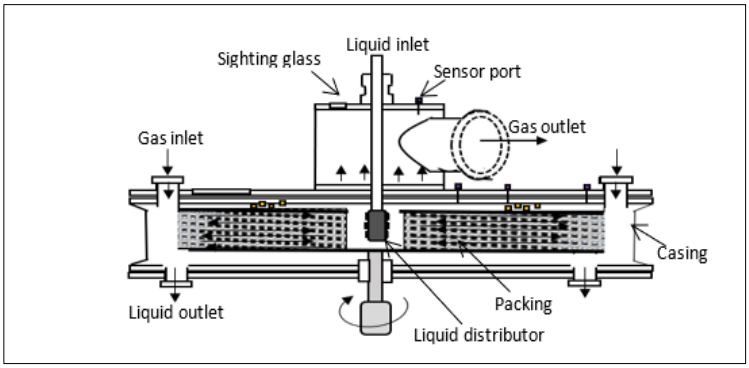

Figure 1: Schematic of a countercurrent flow RPB

Using gas capacity factor (F_G) and liquid load (LL) is one of the many ways of comparing different kinds of equipment. Since, as mentioned above, the least cross-sectional area and centrifugal force occur at the center of the packing where the liquid is injected, the entrainment of liquid is assumed to begin from there (Neumann et al., 2018; Neumann et al., 2017a). F_G is the product of the gas velocity and the square root of the gas density, ρ_G. Thus, the average integrated gas capacity factor ($\bar{F}_G$) and specific liquid load ($\overline{LL}$) are expressed by Groß et al., (2018) as follows:

$$\bar{F}_G = \frac{\dot{V}_G}{2\pi(r_o - r_i)h_p} ln\left(\frac{r_o}{r_i}\right)\sqrt{\rho_G} \quad (1)$$

Similarly, the specific liquid load ($\overline{LL}$)) is given by:

$$\overline{LL} = \frac{\dot{V}_L}{2\pi(r_o - r_i)h_p} ln\left(\frac{r_o}{r_i}\right) \quad (2)$$

Where $\dot{V}_G$ and $\dot{V}_L$ are the volumetric gas and liquid flowrates in respectively, r_i and r_o are the inner and outer radius of the packing respectively, while h_p is the axial height of the packing.

Groß et al., (2020) posited that expressing the rotation speed of RPBs in terms of the high gravity factor (or relative centrifugal force) to compare rotor dimensions is advantageous. The high gravity factor (β) is defined as the ratio of centrifugal acceleration to gravitational acceleration ($\beta = \omega^2 r/g$). Where ω represents the angular rotating speed ($rads^{-1}$), r is the radius (m), and g is the gravitational acceleration. However, at a constant ω, β changes along the radial direction, r. To cater for the change, β is replaced by the average high gravity factor $\bar{\beta}$, which is the magnitude of the centrifugal force from the inner to the outer radius of the rotor given by Zhang et al., (2011) as:

$$\bar{\beta} = \frac{\int_{r_i}^{r_o} 2\beta r dr}{\int_{r_i}^{r_o} 2\pi r dr} = \frac{2\omega^2(r_i^2 + r_i r_o + r_o^2)}{3(r_i + r_o)g} \quad (3)$$

To investigate RPB hydrodynamics such as floodings, entrainment, and variations in pressure drop with changing operational parameters such as, $\bar{\beta}$, $\bar{F}_G$ and $\overline{LL}$, physical visualization method was used by several researchers (Burns et al., 2000; Neumann et al., 2017a). The typical procedure is to keep two operating variables constant and manipulate the third one (Neumann et al., 2017a). It is possible to carry out two procedures to reconfirm the results. The gas flow rate may be set to a constant value, then gradually increased until an excessive liquid splash is observed in the center of the rotor. Increasing beyond a specific limit will make the liquid accumulate in the center of the rotor. To adequately analyze fluid flow behavior in RPBs, (Burns & Ramshaw, 1996) recommended using a combination of visual and quantitative methods. Additionally, Neumann et al., (2017a) have noted that using visual observations and measuring pressure drop fluctuations alone are insufficient to anticipate hydrodynamic behavior in RPBs due to the observed inconsistencies mentioned earlier. In order to determine the operating limits in RPBs, (Burns & Ramshaw, 1996) employed liquid holdup, and (Hendry et al., 2020) used the measurement of the flow rate of the entrained liquid expelled from the center of the rotor.

Figure 2 shows a typical pressure drop against the rotor speed curve and a depiction of the liquid behaviour during RPB operation. A steady increase in pressure drop is obtained at low rotational speeds (usually at $\bar{\beta} \ll 50$). This range is marked by significant liquid entrainment and consequent ejection from the center of the rotor. Severe fluctuations in the pressure drop also mark this range due to liquid ejection. At moderate rotation speeds, the pressure drop reaches a maximum and begins to reduce.

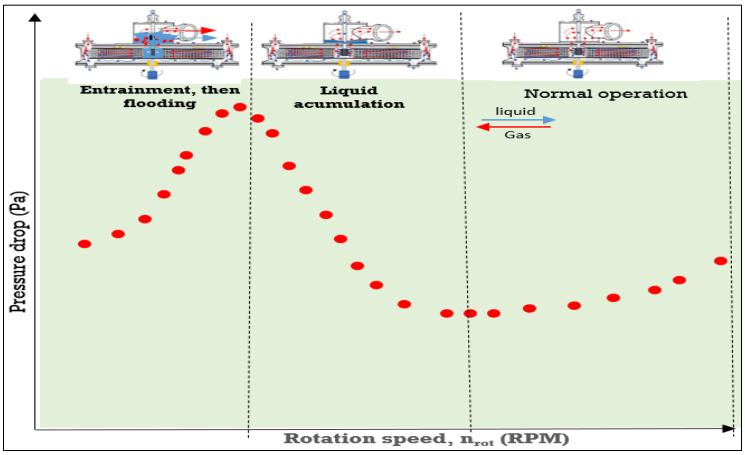

Figure 2: Pressure drop variation with rotation speed in RPB operation

This range is marked by an accumulation and circulation of the liquid in the center of the rotor. At higher rotation speed ($\bar{\beta} \geq 50$), regular operation of the RPB is observed, accompanied by the absence of liquid accumulation in the center of the rotor and a stable pressure drop (Neumann et al., 2017a).

The RPB packing is its core component. Several types of RPB packings have been highlighted by Zhang et al., (2011). The excellent mass transfer characteristics of stainless steel wire mesh packing made it a commonly used RPB packing. Pressure drops for unstructured stainless steel packings made by rolling the wire mesh layer by layer without linkages between the layers, however, lead to lowered efficiencies in production and capacities. To evenly distribute the liquid across the packing, nozzles placed at the center of the packing are used. The nozzles do not rotate and are typically made up of single or multiple perforated pipes. Wang et al., (2019) had reported that the behavior of liquid flow in RPB packings is greatly determined by the structure of the liquid distributor used and identified three classes of liquid distributors for liquid mixing in RPBs: nozzle distributors, premixed distributors, and impinging stream distributors.

Experimental setup and procedure

The experimental setup is shown in Figure 3. RPB500 from Proceller®, Poland was used. The RPB is located at the Laboratoire de Génie Chimique (LGC), Toulouse. To our knowledge, this is the only academic equipment of this type in France for now. The RPB used was a single-stage, vertical rotor type with a casing diameter of 676mm, an inner rotor diameter of 160mm, and an outer rotor diameter of 500mm. The packing was a conventional, multi-layered, single-block stainless steel wire mesh of axial height of 40mm, a specific surface of 2400m^2/m^3, and a porosity of 86%. Two sight glasses placed directly above the center of the rotor and another on the casing made physical, visual observation possible. An air-water system was used. The liquid was sprayed from the center of the RPB using two different types of liquid distributors (see Figures 4c and d). The first liquid distributor used was a dual jet nozzle, flat fan liquid distributor (EUS 1/4 MC3E-20-80 SS316) covering flowrates of 0.38 to 2.4m^3/h. The second was a single pipe liquid distributor, which had 32 x Φ1.5mm holes drilled in 4 rows on 8 equal surface zones of the pipe circumference. The liquid flow rate was measured with a panel-type rotameter. The liquid was recirculated to the feed tank using a by-pass line. Air supply from the general laboratory compressor was used. A pressure sensor connected to a pressure transmitter was placed to measure the pressure drop between the packing periphery and the gas outlet. Pressure drop was

measured over the RPB after stable operating conditions were obtained and remained stable for about four minutes. For each run, pressure drop was measured every 5 seconds for two minutes. The measurement was done in real-time by interfacing the sensors to a computer using the DASYLab data acquisition system (V9.00.02) and analyzed using MATLAB (R2022a) software.

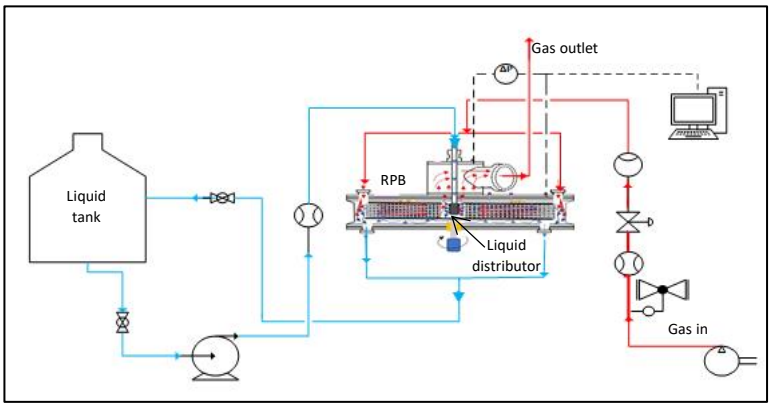

Figure 3: RPB countercurrent process flow diagram

To investigate the hydrodynamic characteristics of the RPB, the three process parameters considered were varied systematically. In each experiment, only one of the parameters was changed at a time, keeping the other parameters constant. The ranges of the parameter studied were as follows: rotation speed from 0 to 1500 rpm, gas flow rate 100-300m_{norm}^3/h, and liquid flow rate 0.39-0.75m^3/h. These ranges correspond to $\bar{\beta}$, $\bar{F}_G$ and $\overline{LL}$ of 0-452, 0.84-2.64$Pa^{0.5}$, and 10-20$m^3m^{-2}h^{-1}$, respectively. A photo of the arrangement is shown in Figure 4. In the dry pressure drop measurements, the frictional pressure drop was first measured by passing air at 100 $m_{norm}{}^3$/h through the stationary rotor and then measuring the pressure drop. The experiment was repeated by increasing the airflow rate in steps 50 $m_{norm}{}^3$/h. The same procedure was repeated with the rotor at various rotation speeds.

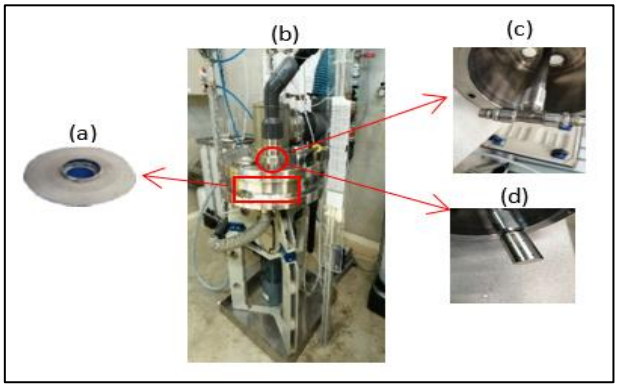

Figure 4. Experimental set up (a) stainless-steel wire mesh packing (b) Photo of RPB pilot (c) double jet liquid (d) single central liquid distributor

Next, the effect of the rotation speed was investigated, initially via the centrifugal pressure drop. In the absence of liquid flow and gas flow, the rotor was set to an initial speed of 100 rpm. The rotation speed was subsequently changed step-wise. The effect of rotation speed was further investigated by varying the rotation speed at constant gas flow rates. For the wet pressure drop, rotation speeds and liquid flow rates were kept constant while the gas flowrate was varied step-wise. In the next set of experiments, the converse of the previous experiment was performed with the liquid flowrate varied step-wise. To investigate the impact of liquid distributor type, for each of the liquid distributors, wet pressure drop experiments as described above were conducted using identical process parameter ranges. To avoid the possible influence of entrained liquids in the centre of the rotor, these set of experiments were conducted within the normal operating range ($\bar{\beta} \geq 50$) of the RPB only.

Results and discussion

Figure 5(a) shows that pressure drop increases with $\bar{\beta}$ at constant $\bar{F}_G$. A slow increase in pressure drop was obtained at low $\bar{\beta}$ values of 50 to 60. At $\bar{\beta}$ values above 65, a rapid and almost linear increase in pressure drop was obtained. This phenomenon may be due to the greater need to overcome the centrifugal head at higher rotational speeds, which consequently causes the air in the rotor and between it and the casing to rotate. The average increase in pressure drop per unit increase in $\bar{\beta}$ in the range investigated was approximately 0.75Pa. This shows that centrifugal pressure contributes significantly to the total dry packing pressure drop. Figure 5(b) also shows a substantially linear increase in pressure drop with increase in $\bar{F}_G$. The phenomenon is caused mainly by gas inertia and drag force. On average, Figure 5(b) shows that the average increase in pressure drop per unit increase in $\bar{F}_G$ was 4.0Pa. Comparing Figures 5(a) and (b), based on per unit operation parameter, $\bar{F}_G$ influences the dry pressure drop of the RPBs more than $\bar{\beta}$. The trends and ranges of these data agree with the findings of Neumann et al., (2017b) for dry pressure drop in RPBs.

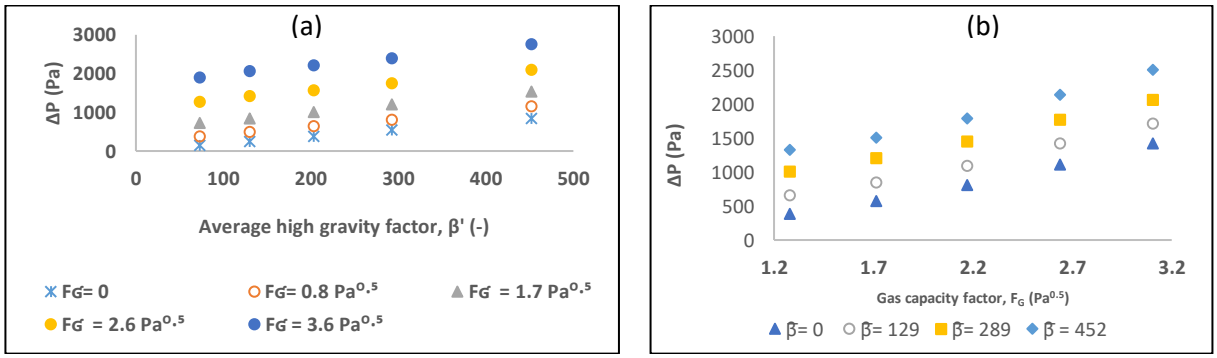

Figure 5: Dry bed pressure drop (a)effect of average high gravity factor (b)effect of gas capacity factor

Figures 6(a) and (b) for the irrigated bed show that the pressure drop variation trend for the wet bed was almost similar to that of the dry bed, with the pressure increasing with an increase $\bar{\beta}$ and with the $\bar{F}_G$. Liu et al., (2018) identified the drenching of the packing surface, which affects the frictional pressure drop, and the liquid's obstruction of the packing pores to the flow of gas as the two significant factors that contribute to the increase in pressure drop in wet RPBs. Per unit $\overline{LL}$ increase, Figure 6(b) shows that the average pressure drop increase was far lower than that caused by $\bar{\beta}$ and $\bar{F}_G$. These results confirm the trends and pressure drop ranges obtained in the work of Neumann et al., (2017).

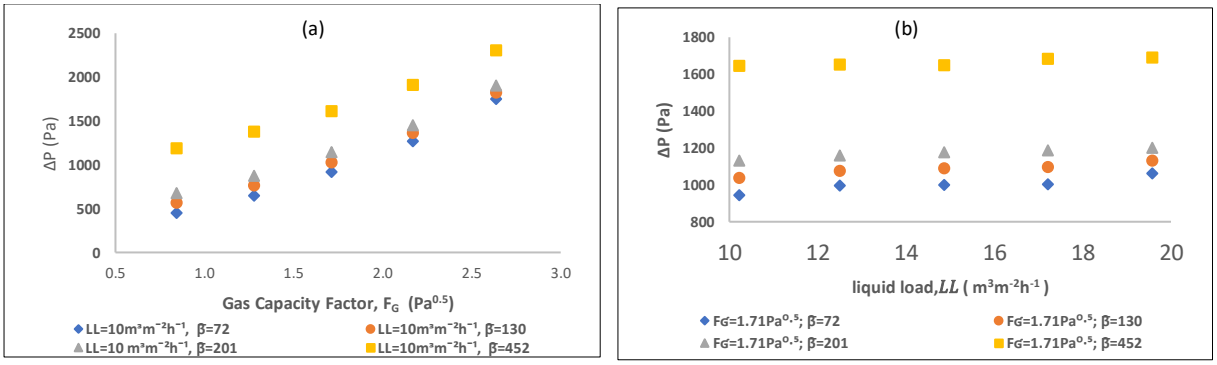

Figure 6: Wet bed pressure drop (a) effect of gas capacity factor (b) effect of liquid load

Figure 7(a) shows that variation in pressure drop with change in $\bar{\beta}$ at constant constant $\overline{LL}$ and $\bar{F}_G$ follows a typical RPB pressure drop variation curve with rotation speed as explained under Figure 2 for the normal operating range. As explained earlier, decreasing the $\bar{\beta}$ forced rotation of air inside and between the rotor and the casing. At high $\bar{\beta}$ values, the regular operation of the RPB was obtained with no liquid entrainment, and the pressure drop was mainly steady. As the pressure drop increased steadily as it was reduced, the presence of water is visually observable in the rotor eye. A further decrease in $\bar{\beta}$ value below 60 reduces the pressure drop and then, after a plateau, increases again

slightly. For a $\bar{F}_G$ of 1.71Pa$^{0.5}$, an almost 90% increase in value $\overline{LL}$ from 10 to 19 m^{3}m^{-2}h^{-1}, produces a moderate increase in the pressure drop with the increase in $\bar{\beta}$, showing the influence of the gas flow in the RPB is more significant than that of the liquid flows.

Figure 7(b) shows the influence of the liquid distributor type when the RPB was operated without liquid accumulation or entrainment. The double jet nozzle (DJ) produced marginally higher pressure drops than the single central (SC) distributor. This phenomenon is attributable to the shorter trajectory traveled by the liquid before entering the packing as total jets, without fragmenting, when the DJ is used.The distance gives the fluids higher kinetic energy and deeper deployment along the axial length of the packing, thus higher pressure drop. The shorter trajectories may be advantageous for mass transfer purposes.

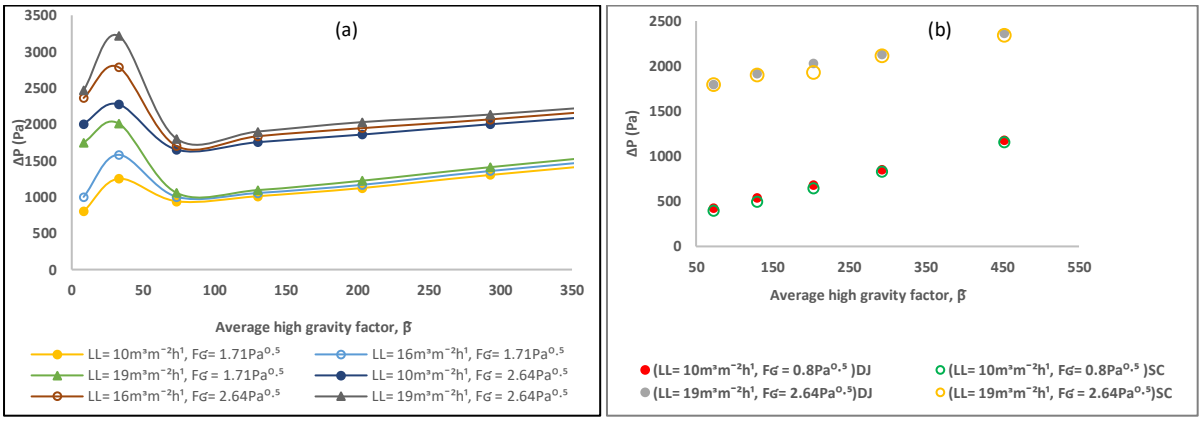

Figure 7: (a) Effect of rotation speed at constant gas capacity factor and liquid load (b) comparing double jet (DJ) and single central (SC) liquid distribtors on pressure drop

Conclusion and Perspective

The hydrodynamics of a pilot-scale RPB equipped with a stainless steel wire mesh packing utilized as a gas/liquid contactor were studied. The maximum value of the average high gravity factor used was 452, integrated gas capacity factor 2.6Pa$^{0.5}$, and a liquid load of up to 20m^{3}m^{-2}h^{-1} were explored. Pressure drops in the RPB investigated were influenced by the three operational parameters: integrated gas capacity factor, average high gravity factor, and liquid loads. Within the normal operating range investigated, a single central liquid distributor produced lower wet pressure drops than a double jet liquid distributor. These investigations will be further explored by developing a novel RPB packing based on the pressure drop data from this work. The new packing geometry will consider a constant liquid holdup through the axial length of the packing. The interfacial area of the 3D printing-based packing will also be measured using a CO_2–NaOH absorption system.

Acknowledgment

This work is conducted under support funding from Overseas Scholarship Scheme (OSS) of Petroleum Technology Development fund (PTDF), Nigeria (Grant Number: PTDF/ED/OSS/PHD/UG/1543/19).

References

Burns, J. R., & Ramshaw, C. (1996). Process intensification: Visual study of liquid maldistribution in rotating packed beds. Chemical Engineering Science, 51(8), 1347–1352. https://doi.org/10.1016/0009-2509(95)00367-3

Burns, J. R., Jamil, J. N., & Ramshaw, C. (2000). Process intensification: Operating characteristics of rotating packed beds - determination of liquid hold-up for a high-voidage structured packing. Chemical Engineering Science, 55(13), 2401–2415. https://doi.org/10.1016/S0009-2509(99)00520-5

Cortes Garcia, G. E., van der Schaaf, J., & Kiss, A. A. (2017). A review on process intensification in HiGee distillation. *Journal of Chemical Technology and Biotechnology*, *92*(6), 1136–1156. https://doi.org/10.1002/jctb.520

Górak, A. (2015). and Chemical Engineering bio , micro , hybrid , cylic , high gravity : Andrzej Górak. *Https://Efce.Info/Efce_media/-p-8976*. https://efce.info/efce_media/-p-8976

Groß, K., De Beer, M., Dohrn, S., & Skiborowski, M. (2020). Scale-Up of the Radial Packing Length in Rotating Packed Beds for Deaeration Processes. Industrial and Engineering Chemistry Research, 59(23), 11042–11053. https://doi.org/10.1021/acs.iecr.0c00868

Groß, K., Neumann, K., Skiborowski, M., & Górak, A. (2018). Analysing the operating limits in high gravity equipment. Chemical Engineering Transactions, 69, 661–666. https://doi.org/10.3303/CET1869111

Hendry, J. R., Lee, J. G. M., & Attidekou, P. S. (2020). Pressure drop and flooding in rotating packed beds. *Chemical Engineering and Processing - Process Intensification*, *151*(March), 107908. https://doi.org/10.1016/j.cep.2020.107908

Hilpert, M., & Repke, J. U. (2021). Experimental Investigation and Correlation of Liquid-Side Mass Transfer in Pilot-Scale Rotating Packed Beds. *Industrial and Engineering Chemistry Research*, *60*(14), 5251–5263. https://doi.org/10.1021/acs.iecr.1c00440

Liu, X., Jing, M., Chen, S., & Du, L. (2018). Experimental study of gas pressure drop in rotating packed bed with rotational-stationary packing. *Canadian Journal of Chemical Engineering*, *96*(2), 590–596. https://doi.org/10.1002/cjce.22936

Neumann, K., Gladyszewski, K., Groß, K., Qammar, H., Wenzel, D., Górak, A., & Skiborowski, M. (2018). A guide on the industrial application of rotating packed beds. *Chemical Engineering Research and Design*, *134*, 443–462. https://doi.org/10.1016/j.cherd.2018.04.024

Neumann, K., Hunold, S., Groß, K., & Górak, A. (2017a). Experimental investigations on the upper operating limit in rotating packed beds. *Chemical Engineering and Processing: Process Intensification*, *121*(August), 240–247. https://doi.org/10.1016/j.cep.2017.09.003

Neumann, K., Hunold, S., Skiborowski, M., & Górak, A. G. (2017b). *Dry Pressure Drop in Rotating Packed Beds Systematic Experimental Studies*. https://doi.org/10.1021/acs.iecr.7b03203

Pan, S. Y., Wang, P., Chen, Q., Jiang, W., Chu, Y. H., & Chiang, P. C. (2017). Development of high-gravity technology for removing particulate and gaseous pollutant emissions: Principles and applications. *Journal of Cleaner Production*, *149*, 540–556. https://doi.org/10.1016/j.jclepro.2017.02.108

Wang, Z., Wu, X., Yang, T., Wang, S., Liu, Z., & Dan, X. (2019). Droplet characteristics of rotating packed bed in H2S absorption: A computational fluid dynamics analysis. *Processes*, *7*(10), 1–29. https://doi.org/10.3390/pr7100724

Zhang, L. L., Wang, J. X., Xiang, Y., Zeng, X. F., & Chen, J. F. (2011). Absorption of carbon dioxide with ionic liquid in a rotating packed bed contactor: Mass transfer study. *Industrial and Engineering Chemistry Research*, *50*(11), 6957–6964. https://doi.org/10.1021/ie102597

Zhang, W., Xie, P., Li, Y., Teng, L., & Zhu, J. (2020). Hydrodynamic characteristics and mass transfer performance of rotating packed bed for CO2 removal by chemical absorption: A review. *Journal of Natural Gas Science and Engineering*, *79*(May), 103373. https://doi.org/10.1016/j.jngse.2020.103373